

## PAPER

View Article Online  
View Journal | View IssueCite this: *Green Chem.*, 2020, **22**, 4561

# Biosourced terpenoids for the development of sustainable acrylic pressure-sensitive adhesives *via* emulsion polymerisation†

Martijn A. Droesbeke,<sup>a</sup> Alexandre Simula,<sup>b</sup> José M. Asua<sup>b</sup> and Filip E. Du Prez<sup>b</sup>  <sup>\*,a</sup>

The increasing regulations and restrictions in favour of a biobased and sustainable community could potentially harm the strong economic position of the polymer industry, which still heavily relies on crude oil. The adhesive industry, in particular, is looking for more renewable alternatives and more environmentally friendly synthesis routes. In this work, (meth)acrylate derivatives of terpenoids, namely tetrahydrogeraniol, citronellol, menthol and isoborneol are introduced in the synthesis of waterborne pressure-sensitive adhesives (PSA) based on acrylic latexes *via* emulsion polymerisation. This industrially implemented setting enables the preparation of five different formulations with high biobased content with a renewable carbon content ranging from 70 to 100%. The biobased PSAs are found to be comparable in terms of tack, peel strength and shear resistance to a benchmark petroleum-derived commercial product. They show good adhesion properties on steel, glass and polyethylene surfaces. Moreover, the various formulations displayed different mechanical and adhesion properties, which make them attractive for a wide range of applications.

Received 17th April 2020,  
Accepted 18th June 2020

DOI: 10.1039/d0gc01350a

rsc.li/greenchem

## Introduction

Pressure-sensitive adhesives (PSAs) are soft polymeric materials that show permanent stickiness at room temperature and instantly adhere to surfaces when mild pressure is applied.<sup>1–4</sup> These viscoelastic materials need a good balance between viscosity and elasticity to ensure wettability and adherence to the substrate surface, while ensuring a certain holding power and clean removal after use. The adhesion performances can be regulated by the copolymer formulation, which will determine the glass transition temperature ( $T_g$ ) and the shear modulus ( $G$ ). Acrylic PSAs have the highest market share among all PSAs, with a yearly production of 1.7 MT (of 3.1 MT in total) with an expected yearly growth rate of 5%.<sup>5</sup> Their increased oxygen, UV and heat resistance, as well as their ability to be manufactured according to the consumer need by simply adjusting the monomer formulation of the

copolymer, maintaining a low additive level, explains their popularity.<sup>1–3</sup>

Typically, an acrylic PSA consists of 70 to 90% of a “soft” acrylate (*e.g.* 2-ethylhexyl acrylate). A high amount of such monomer is needed to bring the  $T_g$  of the material down to values ensuring a good tack, typically between  $-5\text{ }^{\circ}\text{C}$  and  $-60\text{ }^{\circ}\text{C}$ .<sup>1–3</sup> To ensure elasticity and strength of the joint, 10 to 30% of a “hard” acrylate (*e.g.* methyl methacrylate) is built in to increase the final  $T_g$ .

However, the adhesives industry is highly dependent on finite fossil resources and their solvent-based polymerisation methods leading to adhesive materials with volatile organic compounds (VOCs). This dependence is an increasing concern in today's environmentally conscious society.<sup>6–10</sup> Due to the anticipated limitations in the crude oil reserves and the design of policy-influencing documents in favour of a biobased and sustainable economy,<sup>5,7</sup> the industry is forced to seek greater sustainability both in resource and in processes<sup>8,11–15</sup> without compromising the properties of the end-products.

In the past years, several reports on new and more renewable building blocks for PSAs have been published. Imam *et al.*<sup>16</sup> and Vendamme *et al.*<sup>6</sup> combined all these studies and provided a detailed overview, where examples of fatty acids,<sup>17–19</sup> starch-derived<sup>20,21</sup> building blocks or a combination<sup>22</sup> thereof can be found. The roll of catechol in nature as a adhesion promotor has also been a source of inspiration for adhesive systems.<sup>23–25</sup> Next to these resources, terpenes prove

<sup>a</sup>Polymer Chemistry Research group, Centre of Macromolecular Chemistry (CMaC), Department of Organic and Macromolecular Chemistry, Faculty of Sciences, Ghent University, Krijgslaan 281-S4bis, B-9000 Ghent, Belgium.

E-mail: Filip.Duprez@UGent.be

<sup>b</sup>Kimika Aplikatua Saila, Kimika Zientzien Fakultatea, Joxe Mari Korta Zentroa, POLYMAT, University of the Basque Country UPV/EHU, Tolosa Hiribidea 72, 20018 Donostia-San Sebastián, Spain

†Electronic supplementary information (ESI) available. See DOI: 10.1039/d0gc01350a

to be a wide and diverse class of renewable organic compounds that include a large structural and functional variety.<sup>26–28</sup> Their successful incorporation in various applications<sup>8,11,15</sup> such as coatings,<sup>29</sup> resins<sup>30</sup> and thermoplastic elastomers<sup>31</sup> and their easy modification into reactive monomers<sup>29,32,33</sup> have demonstrated their viability in commercial products. Therefore, these compounds appear as good candidates for the market of biosourced PSAs. Their large structural variety gives a whole library of building blocks that allow to tune the  $T_g$  of the PSA copolymer and therefore its adhesive performance.

The use of terpenes in acrylic PSA applications has already been reported. Baek *et al.* used tetrahydrogeranyl acrylate (THGA) combined with isobornyl<sup>34</sup> or menthyl<sup>35</sup> acrylate, to obtain optically clear pressure-sensitive adhesives *via* UV light-triggered photocopolymerisation in bulk. The use of tetrahydrogeranyl acrylate was also reported in a recent study by Noppalit *et al.*<sup>36</sup> They obtained block copolymers by copolymerising THGA with styrene *via* Reversible Addition-Fragmentation Transfer (RAFT) Polymerisation. By employing this technique, it was shown that the length of the blocks allows adjusting the adhesion-cohesion balance. A similar study was performed *via* Nitroxide Mediated Polymerisation (NMP).<sup>37</sup>

While these reports have encouraged the use of biosourced building blocks in PSAs, other measures will need to be taken to encounter new environmental restrictions and regulations, avoiding solvent-based adhesives and energy-consuming techniques such as solution or bulk polymerisations.<sup>5–7,38</sup> Therefore, the radical polymerisation of biobased monomers in dispersed aqueous media is getting a lot of attention.<sup>6,39,40</sup> The use of a wide selection of raw materials, the better control of the final product properties and the usage of water as a benign solvent, offer indeed higher compliance with new environmental guidelines. Large contributors to this renewable and sustainable field are fatty acids<sup>39,41–44</sup> as they provide soft monomers, which attracted the attention of both industry and academic world.<sup>45–50</sup> Recently, a study on the emulsion polymerisation of eugenol, a lignin derivative providing hard building blocks for adhesive applications, was published.<sup>51</sup>

On the other hand, terpene-based chemicals have the potential of becoming more important as an alternative to both soft and hard monomers.<sup>36</sup> Recently, Noppalit *et al.*<sup>52</sup> obtained sustainable, waterborne pressure-sensitive adhesives using terpene-based triblock copolymers *via* RAFT polymerisation in mini-emulsion. This study complies with the new environmental guidelines, but mini-emulsion polymerisation is an energy intensive technique, whose industrial use is only justified for materials that cannot be produced otherwise, mostly for hybrid (polymer-polymer and polymer-inorganic) waterborne dispersions.<sup>40,53,54</sup> Although the use of emulsion polymerisation for very hydrophobic monomers is challenging,<sup>42</sup> it is worth to explore this technique for the synthesis of terpene-based waterborne PSAs.

Studies have already been reported on emulsion polymerisation and copolymerisation of terpenes such as myrcene,<sup>55–59</sup>

alloocimene<sup>60</sup> and the commercially available isobornyl (meth)acrylate (iBn(M)A).<sup>61</sup> However, reports within the field of acrylic PSA are only limited to the use of a specific terpene-based building block for acrylic PSA applications *via* emulsion polymerisation, as published by Badia *et al.*<sup>62,63</sup> and Zhang *et al.*<sup>64</sup> Both described the use of iBnMA as the hard monomer combined with 2-octyl acrylate as a fatty acid-derived soft monomer and butyl acrylate, thus obtaining a fully and partially biobased PSA latex, respectively. Zhang *et al.* also reported that iBnMA has a positive effect on the PSA performance as it increases the spacing between the chains, increasing the wetting and thus the adhesion property of the PSA.

In the present work, the main aim is to broaden the range of terpenoids used in the field of acrylic PSAs prepared by emulsion polymerisation, with renewable alternatives for both soft and hard monomers. In this context, the investigation of fully terpene-based acrylic PSAs with a high biobased content will be described. More specifically, the (meth)acrylate derivative of four common terpenoids, being tetrahydrogeraniol, citronellol, menthol and isoborneol, were combined with methyl methacrylate (MMA) and acrylic acid (AA) (Fig. 1), two monomers that are generally used in the adhesive industry to create terpene-based acrylic waterborne PSAs with biosourcing potential.<sup>65–67</sup> The most sustainable modification of terpenoids into (meth)acrylates was already described in a preceding study.<sup>33</sup> Herein, the seeded semi-batch emulsion polymerisation of those biobased acrylic terpenoids to obtain



Fig. 1 The structure of 2-ethyl hexyl acrylate, the four terpene-based (meth)acrylate monomers combined with acrylic acid and methyl methacrylate used in the PSA formulations. \*The values for  $T_g$  were adopted from Sigma-Aldrich.

acrylic PSA latexes with a high biobased content, is reported. Tetrahydrogeranyl acrylate is believed to be a biobased, soft monomer being alternative to 2-ethyl hexyl acrylate, while isobornyl and menthyl methacrylate can be valuable biobased hard monomers to replace MMA. Citronellyl (meth)acrylate was thought of as a bifunctional biobased monomer for promoting crosslinking during radical polymerisation. The adhesion-cohesion balance of the fully biobased and terpenoid-based adhesive material was assessed *via* rheology testing to study the shear modulus. On the other hand, the adhesive performance was determined *via* tack, peel and shear experiments on different surfaces in an attempt to match crude-oil based PSAs and to investigate the influence of the formulation on the final properties. This study could lead to high repercussions on the PSA industry as it could provide a direct industrial implementation of terpenoid-based monomers in the production of fully biobased, waterborne acrylic PSAs.

## Results and discussion

In order to conduct this study, the starting point was a non-biobased waterborne acrylic latex-based PSA (**PSA1**) (Table 1)<sup>68</sup> acting as an crude oil-based benchmark. The latter consists of 2-ethyl hexylacrylate (2EHA), methyl methacrylate (MMA) and acrylic acid (AA), all highly used monomers in PSA industry.

The physical properties of the prepared PSA, namely the particle size (dp), the solid weight content (SWC), the gel content, the thermal properties and the biobased content or renewable carbon content (RCC) connected to the used monomers with their weight ratio, are presented in Table 1. The gel content, which was determined *via* soxhlet extraction, is related to the crosslinked fraction in the pressure-sensitive adhesive and its value gives an indication on the cohesive properties of the PSA. The SEC data of the soluble fraction are reported in Table S5.† The gel content is directly linked to the shear modulus and therefore to the final properties of the material. Methyl methacrylate is used in this formulation as a hard monomer and should also reduce the amount of intermolecular chain transfer, a common phenomenon in the radical polymerisation of acrylates.<sup>69–73</sup> The addition of MMA

will decrease the amount of branching and crosslinking and thus reduce the gel fraction. The pendant carboxylic acid present in the acrylic acid is utilised to increase the wetting of the adhesive to the surface and to improve the cohesiveness of the PSA.<sup>2</sup> A certain percentage of these two monomers is therefore desired in PSA formulations. Five waterborne terpenoid-based latexes were designed to compare their performance to the crude oil-based **PSA1** with similar physical properties in terms of particle size, SWC of the latex and  $T_g$  (Table 1).

To improve the RCC of **PSA1**, 2EHA was replaced with a biobased alternative, *i.e.* tetrahydrogeranyl acrylate (THGA) in **PSA2**. In this way, the RCC was increased to 100% as MMA and AA can be produced from natural sources and therefore were considered as biobased during this study.<sup>66</sup> The terpenoid-based acrylate THGA was chosen as DSC analysis showed that the  $T_g$  of pTHGA is in the same range as the one of p2EHA (−73 °C for pTHGA and −50 °C for p2EHA) (Fig. S1†).

The ability of crosslinking in emulsion polymerisation systems in order to increase the cohesion, is well-known.<sup>4,74</sup> Therefore, citronellyl acrylate (CA), with a second unsaturation, was used as a promoter for additional branching and crosslinking, without influencing the final  $T_g$  (Table 1 and Fig. S2†). Citronellyl acrylate possesses allylic hydrogens, which are susceptible to hydrogen abstraction. This abstraction results in a new radical centre at the other end of the citronellyl acrylate, which may be an additional source of branching and crosslinking during polymerization. CA was incorporated in the formulations at 2 wt% (**PSA3**) and 4 wt% (**PSA4**), to increase the gel content (Table 1).

In a next formulation (**PSA5**), isobornyl methacrylate ( $T_g(\text{piBnMA}) = 155\text{ °C}$ )<sup>64</sup> was incorporated in combination with MMA as hard segment precursor in order to determine its effect on the adhesive performance.<sup>61</sup> The monomer iBnMA was considered as 100% biobased in this study as it can be synthesised from isoborneol, also a terpenoid, and biobased MAA.<sup>33,66</sup> Next to iBnMA, the methacrylate counterpart of CA was included in an attempt to potentially decrease the branching and the crosslinking density of the resulting PSA as a methacrylate. However, the results indicate no real difference on the gel content between **PSA3**, **PSA4** and **PSA5** (between 92 and 96%). At this stage, except a slight difference in the  $T_g$

**Table 1** Summary of the properties of the different PSA latexes

PSA	Monomer formulation	Weight ratio	dp <sup>a</sup> (nm)	SWC <sup>b</sup> (%)	Gel <sup>c</sup> (%)	$T_g$ (°C)	$T_{d, 5\%}$ <sup>d</sup> (°C)	RCC <sup>e</sup> (%)
1	2EHA : MMA : AA	84 : 14 : 2	121 ± 2	41	74 ± 0	−43	344	16
2	THGA : MMA : AA	84 : 14 : 2	128 ± 1	41	76 ± 1	−42	333	100
3	THGA : CA : MMA : AA	82 : 2 : 14 : 2	119 ± 1	41	92 ± 0	−40	323	100
4	THGA : CA : MMA : AA	80 : 4 : 14 : 2	111 ± 1	43	95 ± 0	−40	336	100
5	THGA : CMA : iBnMA : MMA : AA	80 : 4 : 7 : 7 : 2	110 ± 1	44	96 ± 0	−34	302	100
6	THGA : MnMA : AA	84 : 14 : 2	162 ± 9	40 <sup>f</sup>	57 ± 4	−43	320	100

<sup>a</sup> Particle size determined by dynamic light scattering (DLS). <sup>b</sup> Solid weight content determined *via* gravimetry. <sup>c</sup> Gel fraction was determined by Soxhlet extraction in THF. <sup>d</sup> TGA thermograms can be found in Fig. S3.† <sup>e</sup> Renewable carbon content (RCC) was calculated considering 100% biobased iBnMA, MMA and AA since these compounds can all be produced from natural resources, although the synthesis method of the commercial monomers used in this work is not known here.<sup>65–67</sup> <sup>f</sup> An SWC of 40% was reached after water evaporation from the latex synthesised *via* batch emulsion polymerisation.

value, no significant effect can be attributed to the presence of iBnMA. Nevertheless, **PSA5** was taken up further to study the influence of iBnMA on the viscoelastic properties of the resulting biobased material (*vide infra*).

In a final formulation, iBnMA and MMA have been substituted with menthyl methacrylate ( $T_g(\text{pMnMA}) = 76\text{ }^{\circ}\text{C}$ ) (Fig. S1†), a hard terpenoid-based monomer that allowed reaching a similar  $T_g$  as **PSA1**. The resulting **PSA6** can be considered as an almost fully terpenoid-based material (98%) as it has to contain 2% of AA necessary for the adhesive performance. The reasoning behind the study of **PSA6** was that the pendant menthyl group could have the same positive impact on the bonding process as iBnMA with a decrease in  $T_g$  compared to **PSA5** (Table 1).

The PSA latexes were synthesised using seeded semi-batch emulsion polymerisation. This technique is frequently applied in industrial context in order to obtain a waterborne, high SWC latex and larger particle size. In order to synthesise these latexes, first a batch emulsion polymerisation was performed for each formulation to obtain a latex with a particle size of around 80 nm and a SWC of approximately 20%. In the next polymerisation step, the seed particles were then fed with a neat monomer mixture in order to increase both the SWC and the particle size. The feeding was carried out under starved conditions, maintaining the instantaneous conversion above 80% during the whole process for **PSA1** to **PSA5**. This requirement is crucial to obtain copolymers with a homogeneous composition. Fig. 2 shows the instantaneous conversion and the particle growth over time for the seeded semi-batch emulsion polymerisation of **PSA2**. Even though full conversion was not obtained, GC analysis confirmed an equal introduction of each monomer in the final PSA polymer.

The slight discrepancy observed between the theoretical and experimental values of the particle sizes in Fig. 2, may be due to some limited aggregation occurring towards the end of the process. This discrepancy was also observed for **PSA1** to **PSA5** (Fig. S4–S7†). In addition, some secondary nucleation was observed at the beginning of the semi-batch operation in some cases (Fig. S4–S7†). However, these events only occurred to a small extent and stable latexes without coagulum were obtained.

In **PSA6**, iBnMA and MMA are replaced by MnMA. The increased hydrophobicity of the monomer composition, due to the replacement of MMA by MnMA, proved to be problematic even during the synthesis of the seed, as coagulation was observed, and a low monomer conversion was obtained after the batch emulsion polymerisation (data not shown). In a second attempt to synthesise the seed, the diffusion of the hydrophobic monomer through the aqueous phase was promoted by the addition of acetone (up to 10 wt%) to the monomer phase.<sup>37</sup> Acetone was utilised herein as a relatively benign solvent (classified as ‘amber’ solvent in the GSK solvent selection guide)<sup>75</sup> with a good monomer affinity. The low boiling point also ensures a facile removal and recycling after the synthesis, leaving only trace amounts in the final PSA product. Because of this, acetone is commonly used for other

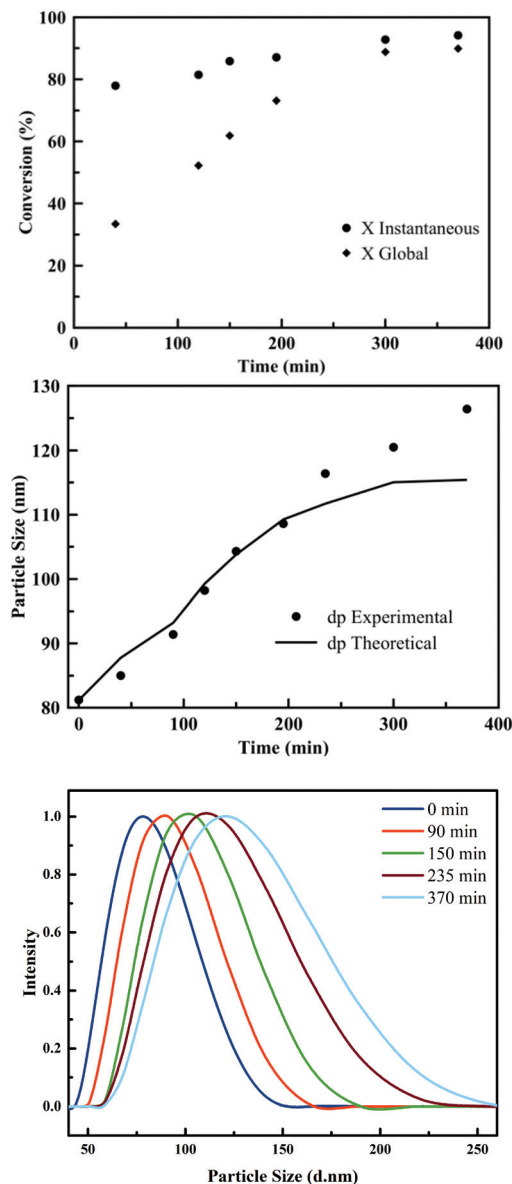


Fig. 2 The conversion as a function of time (top), the evolution of the particle size as a function of time (middle) and the corresponding DLS traces (bottom) of **PSA2** during feeding in the seeded semi-batch emulsion polymerization.

syntheses such as waterborne polyurethanes.<sup>76–78</sup> The addition of acetone resulted in an increase of the monomer conversion (87% after 21 hours of polymerisation) and to the formation of a stable latex that could be employed as a seed. However, the seeded semi-batch emulsion polymerisation was not successful despite the use of acetone, because of the low instantaneous monomer conversion attained (40%) (Fig. S8†). The reason for this low conversion is discussed in the ESI.† One conclusion from this discussion is that conversion could be likely improved by using an emulsion feed. However, in this work it was decided to circumvent the problematic seeded semi-batch emulsion polymerisation by concentrating the seed



latex (SWC = 19%) by rotary evaporation. In this way, the desired SWC (40%) was obtained, in order for the film formation to be comparable to the other PSA latexes. This process is very similar to devolatilization that is industrially used to remove the unreacted monomer from latexes.<sup>79</sup> In this particular case, rotary evaporation might slightly reduce the amount of free monomer in the latex, limiting the plasticization of the PSA6 by the monomer.

For an in-depth understanding of the crosslinking of the various PSA formulations, the combination of Asymmetric Flow Field-Flow Fractionation (AF4) and soxhlet extraction was employed. From the results obtained with AF4, we can conclude that **PSA3**, **PSA4** and **PSA5**, all containing CA or CMA, are fully crosslinked as no low molecular weight polymers can be observed when plotting the evolution of the molar mass as a function of time (Fig. S9†) and the molecular weight distribution (Fig. S10†). Lower molar mass polymers were obtained with **PSA1**, **PSA2** and **PSA6**, indicating that branching occurred, but to a lower extent. These results are comparable to the ones obtained *via* soxhlet extraction.

The mechanical and bonding/debonding behaviour of the studied materials have been initially characterised by rheology using frequency sweep measurements to get a first insight in their performance using Chang's classification for PSAs.<sup>80,81</sup> The storage ( $G'$ ) and loss ( $G''$ ) modulus were therefore measured at  $10^{-2}$  rad s<sup>-1</sup> to  $10^2$  rad s<sup>-1</sup>, the frequencies corresponding with the bonding and debonding step respectively (Fig. 3B). Following Chang's classification of PSAs (Fig. 3A), each formulation can be applied to a specific purpose, depending on the values for  $G'$  and  $G''$ . For instance, **PSA1**, **2** and **6** are

more likely to be applied as "General Purpose PSAs" (labels, tapes, *etc.*), whereas other formulations such as **PSA3**, **4** and **5** could be utilised as "High Shear PSAs".

The PSA properties derived from Chang's classification were confirmed *via* additional rheology measurements. The rheological master curve of  $G'$  was obtained using the time-temperature superposition principle to gain a full insight on the rheological behaviour of the PSA materials (Fig. 4 and Fig. S11–S16†). A higher plateau value of  $G'$  was observed for the formulation classified as High Shear PSAs (Fig. 3B and 4). Moreover, the same two categories were observed in the rheological measurements. On the one hand, the formulations with citronellyl-based monomers, namely **PSA3**, **PSA4** and **PSA5**, exhibiting a higher  $G'$  because of the increased crosslink density and high gel content, and on the other hand, the formulations **PSA1**, **2** and **6** displaying a lower  $G'$  plateau value and a lower gel content. This rheology study also confirms the clear trend between the gel content and the  $G'$  value.

A temperature sweep measurement (Fig. S17†) was also performed to investigate if the materials meet the Dahlquist criterion ( $G' < 3.3 \times 10^5$  Pa) at room temperature (25 °C)<sup>80</sup> as all materials show a high modulus ( $G'$ ). Only **PSA3** and **PSA5** did not meet this empiric criterion with slightly higher  $G'$  values. However, these materials still show potential as high shear PSAs.

To further characterise the adhesive performance of the studied materials, tack, peel and shear measurements were carried out on different surfaces, being stainless steel, glass and polyethylene (PE). Probe and loop tack testing were performed to characterise the initial tack of the PSA to the substrate. Peel tests were performed in a 180° peel setup to measure the peel strength of the PSA. Both tack and peel are related to the adhesion performance of the adhesive. The shear resistance or the resistance to debonding can be related to the cohesion of the PSA and was tested with a Shear Adhesion Failure Tester (SAFT). The failure temperature was measured under a continuous temperature increase, whereas

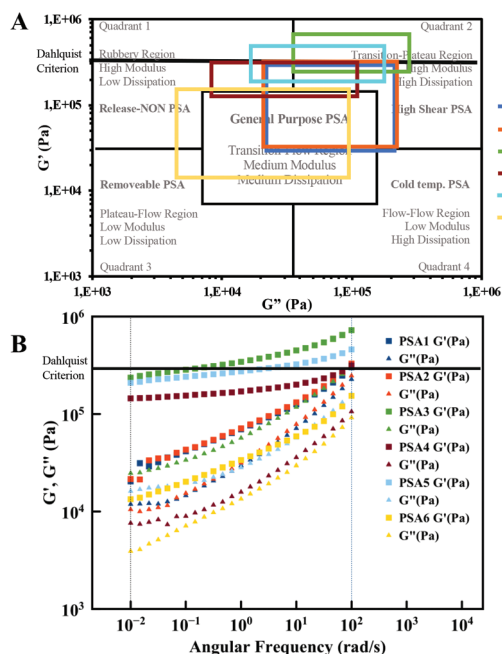


Fig. 3 (A) Chang's viscoelastic window of pressure-sensitive adhesives applied to the synthesised PSAs and (B) frequency sweep measurements performed at room temperature by rheology.



Fig. 4 Rheological master curves of  $G'$  obtained for the different PSA formulations using the time-temperature superposition principle ( $T_{ref} = 25$  °C).

**Table 2** Results of the tack, peel and shear resistance behaviour of the synthesised PSAs on different surfaces

	PSA	Formulation	Peel resistance (N/25 mm)	Tack (N/25 mm)	$W_A^a$ (J m <sup>-2</sup> )	SAFT <sup>b</sup> (°C)	Shear resistance failure time <sup>c</sup> (min)
Steel <sup>d</sup>	1	2EHA : MMA : AA (84 : 14 : 2)	7.6 ± 0.3	6.0 ± 0.5	97.1 ± 4.9	220+	10 000+
	2	THGA : MMA : AA (84 : 14 : 2)	5.9 ± 1.0	4.6 ± 0.6	73.6 ± 10.1	220+	10 000+
	3	THGA : CA : MMA : AA (82 : 2 : 14 : 2)	1.6 ± 0.2	2.3 ± 0.3	34.7 ± 4.7	169 ± 4	10 000+
	4	THGA : CA : MMA : AA (80 : 4 : 14 : 2)	0.6 ± 0.1	1.6 ± 0.3	18.2 ± 2.0	159 ± 2	10 000+
	5	THGA : CMA : iBnMA : MMA : AA (80 : 4 : 7 : 7 : 2)	0.2 ± 0.1	1.4 ± 0.1	14.5 ± 1.3	158 ± 4	10 000+
	6	THGA : MnMA : AA (84 : 14 : 2)	7.7 ± 0.9	5.1 ± 0.8	77.4 ± 11.0	136 ± 2	10 000+
Glass	1	2EHA : MMA : AA (84 : 14 : 2)	6.5 ± 0.9	6.8 ± 0.4	134.5 ± 8.2	191 ± 2	
	2	THGA : MMA : AA (84 : 14 : 2)	5.8 ± 0.6	5.6 ± 0.2	103.3 ± 6.2	213 ± 4	
	3	THGA : CA : MMA : AA (82 : 2 : 14 : 2)	1.2 ± 0.5	2.4 ± 0.2	33.1 ± 1.5	169 ± 8	
	4	THGA : CA : MMA : AA (80 : 4 : 14 : 2)	0.3 ± 0.1	1.6 ± 0.2	21.6 ± 0.8	160 ± 4	
	5	THGA : CMA : iBnMA : MMA : AA (80 : 4 : 7 : 7 : 2)	0.1 ± 0.0	1.4 ± 0.3	16.2 ± 0.7	175 ± 2	
	6	THGA : MnMA : AA (84 : 14 : 2)	5.3 ± 1.2	7.7 ± 0.7	141.2 ± 16.4	53 ± 1	
PE	1	2EHA : MMA : AA (84 : 14 : 2)	3.7 ± 0.9	3.5 ± 0.7	52.0 ± 9.4	96 ± 8	
	2	THGA : MMA : AA (84 : 14 : 2)	3.8 ± 0.4	3.5 ± 0.1	55.7 ± 6.8	94 ± 6	
	3	THGA : CA : MMA : AA (82 : 2 : 14 : 2)	0.3 ± 0.1	1.0 ± 0.1	14.8 ± 0.7	100+	
	4	THGA : CA : MMA : AA (80 : 4 : 14 : 2)	0.0 ± 0.2	0.8 ± 0.1	10.6 ± 1.2	100+	
	5	THGA : CMA : iBnMA : MMA : AA (80 : 4 : 7 : 7 : 2)	0.0 ± 0.0	0.5 ± 0.1	5.7 ± 0.5	100+	
	6	THGA : MnMA : AA (84 : 14 : 2)	6.4 ± 1.9	7.7 ± 1.0	120.8 ± 16.9	49 ± 1	

<sup>a</sup> Work of adhesion, calculated as the area under the curve in a loop tack test. <sup>b</sup> Shear adhesion failure temperature. <sup>c</sup> SAFT measurements, performed as static shear measurements, were stopped after 10 000 min without a cohesive failure, indicating high cohesive forces in all PSA formulations. SAFT measurements can be linked to static shear measurements by introducing an increased temperature in order to decrease the time-scale. This explains why no static shear measurements were performed on glass and PE. <sup>d</sup> Stainless steel.

the failure time was determined under constant temperature. The obtained results are summarised in Table 2.

When the adhesive performance of **PSA1** and **PSA2** are compared on steel surface, no obvious effect was observed after replacing 2EHA by THGA. For **PSA2**, slightly lower but comparable results for tack, peel and shear resistance values (failure temperature and time) were obtained in comparison to **PSA1**. These results indicate that the biobased **PSA2** (RCC = 100%) is similar to the petroleum-based **PSA1** in terms of performance, which confirms the first reports on terpenoids being a viable option for replacing crude oil resources in the synthesis of bio-based acrylic PSAs *via* emulsion polymerisation.<sup>62–64</sup>

The strong interplay between adhesion and cohesion properties of an adhesive is actively linked to the intermolecular forces and crosslinking. Crosslinking increases the gel fraction, which has a positive effect on the cohesion but a negative impact on the adhesion, leading to lower tack and peel values. This effect is confirmed when analysing the formulations containing CA or CMA. The increase of the gel fraction leads to a decrease in peel and tack properties of **PSA3**, **PSA4** and **PSA5**. When the amount of CA was doubled (**PSA4**), the gel content slightly increased and the tack and peel properties further decreased. However, in rheology, the opposite effect is observed. The storage modulus  $G'$  dropped below the Dahlquist criterion (Fig. S16†), which would mean a better adhesion and better tack and peel properties, while the inverse effect is observed herein. This irregularity could be linked to the effect of  $G''$ .  $G''$  is lower for **PSA4** than for **PSA3**, which results in **PSA4** being a less flowing material. A lower wetting of the substrate will result in weaker adhesion properties, leading to lower tack and peel resistance.

Consequently, the internal crosslinking provided in **PSA3** and **PSA4** render the cohesion of the adhesive relatively strong, thus placing the adhesives at the limit of what can be considered as a PSA. The same could be concluded for **PSA5**. The excessive gel content caused a drop in adhesive performance, even in the presence of iBnMA, which is generally seen as an adhesion promotor.<sup>64</sup>

In **PSA6**, a lower gel fraction was obtained. By substituting iBnMA and MMA with MnMA, a positive effect on the tack and peel properties was observed, reaching similar values as **PSA1** and **PSA2** on stainless steel. However, a lower shear adhesion failure temperature indicates a lower cohesion performance in respect to **PSA2**, likely due to the lower gel fraction of **PSA6**. While this interplay is in agreement with the adhesion-cohesion balance of adhesives, the presence of unreacted monomers in **PSA6** could also cause a plasticising effect, influencing the adhesive balance.

Again, during the PSA performance tests, two categories could be considered. The first category (formulations with CA or CMA) will exhibit a higher cohesion property than the second category (formulations without CA or CMA), showing a better adhesion.

The same trend in the adhesive properties was also observed on glass surface. However here, a higher tack and work of adhesion was measured for all PSA formulations on this substrate, while SAFT measurements indicate a decrease in shear resistance. These effects can be attributed to the difference in surface energy between glass (>60 mN m<sup>-1</sup>) and steel (35–46 mN m<sup>-1</sup>).<sup>82,83</sup> The adhesion to PE is generally more challenging for most of the acrylic-based PSAs.<sup>84</sup> However, remarkably, good tack, peel and shear resistance



Fig. 5 Probe tack test results for the six formulations presented in Table 1.

values were observed for **PSA6**. Moreover, the results obtained for **PSA6** on steel, glass and PE, indicate that it can be a valuable PSA material for the adhesive industry.

A similar trend is observed when the materials are tested *via* probe tack measurements. The shape of the curve (dissipation profile) and the peak stress value can be linked to the performance of the PSA. In Fig. 5, a low strain is observed for all PSA formulations, which is expected for general purpose to high shear PSAs as they display high cohesion forces. **PSA1** and **PSA2** have similar peak stress values and dissipation profiles, indicating a similar adhesive behaviour between the bio-based adhesive and its crude oil counterpart, confirming previous observations. It is worth pointing out that the probe-tack curves for **PSA1** and **PSA2** did not present a clear plateau, indicating that these adhesives were too cohesive and the energy needed for fibrillation exceeded that of the detachment from the substrate. The higher gel content in **PSA3**, **PSA4** and **PSA5** resulted in an even more rapid detachment of the adhesive from the substrate because these PSAs were too elastic (high  $G'$ , Fig. 4). The probe-tack curve for **PSA6** showed a quite classical shape with a high level of fibrillation during debonding. However, the stress was low due to the modest gel content of this PSA, and possibly to the presence of some residual monomer.

## Conclusion

In this study, 100% biobased and waterborne pressure-sensitive adhesives from terpenoid-based (meth)acrylates were synthesised through emulsion polymerisation. It was demonstrated that the obtained materials were able to achieve similar properties as those of the non-biobased PSAs. Different formulations were tested in order to determine the property-to-composition relation. Tack, peel and shear resistance measurements showed similar adhesive performance for **PSA2** and **PSA6** compared to **PSA1** on stainless steel and glass. These results were in line with the rheology measurements.

Moreover, all PSA formulations were classified within the General Purpose and High Shear PSA region, indicating their potential commercial relevance. While the adhesive performance on PE was found to be more challenging, as already observed for other acrylic-based PSAs, **PSA6** showed good adhesion to a PE surface, and moreover displayed promising results overall. Finally, we also demonstrated the interesting branching and crosslinking capability of citronellyl (meth)acrylate as a biobased crosslinker.

Together, the results of the present study show that the incorporation of terpenoids in the field of pressure-sensitive adhesives is a valuable option for the creation of a range of more biobased adhesive products.

## Conflicts of interest

There are no conflicts to declare.

## Acknowledgements

The authors would like to acknowledge Dr Nezha Badi and Dr Resat Aksakal for their guidance. We would also like to thank Dr Amaia Agirre for the AF4 measurements.

## References

- 1 C. Creton, *MRS Bull.*, 2003, **28**, 434–439.
- 2 I. Benedek, *Pressure-Sensitive Adhesives and Applications*, CRC Press, 2nd edn, 2004.
- 3 D. Satas, *Handbook of Pressure Sensitive Adhesive Technology*, Springer, US, 2nd edn, 1989.
- 4 A. Zosel, *J. Adhes.*, 1991, **34**, 201.
- 5 Markets and Markets, *Pressure Sensitive Adhesives Market - Global Forecast To 2026*, 2016.
- 6 R. Vendamme, N. Schüwer and W. Eevers, *J. Appl. Polym. Sci.*, 2014, **131**, 8379.
- 7 Ellen MacArthur Foundation, *The New Plastics Economy: Rethinking the future of plastics*, 2016.
- 8 M. N. Belgacem and A. Gandini, *Monomers, Polymers and Composites from Renewable Resources*, Elsevier Science, 2008.
- 9 C. R. McElroy, A. Constantinou, L. C. Jones, L. Summerton and J. H. Clark, *Green Chem.*, 2015, **17**, 3111–3121.
- 10 P. Anastas and J. Warner, *Green Chemistry: Theory and Practice*, Oxford University Press, 2000.
- 11 A. Gandini and T. M. Lacerda, *Prog. Polym. Sci.*, 2015, **48**, 1–39.
- 12 R. P. Wool and X. S. Sun, *Bio-Based Polymers and Composites*, Academic Press, 2005.
- 13 J. J. Bozell and G. R. Petersen, *Green Chem.*, 2010, **12**, 539–554.
- 14 K. Yao and C. Tang, *Macromolecules*, 2013, **46**, 1689–1712.
- 15 Y. Zhu, C. Romain and C. K. Williams, *Nature*, 2016, **540**, 354.

- 16 S. H. Imam, C. Bilbao-Sainz, B.-S. Chiou, G. M. Glenn and W. J. Orts, *J. Adhes. Sci. Technol.*, 2013, **27**, 1972–1997.
- 17 W. Maassen, M. A. R. Meier and N. Willenbacher, *Int. J. Adhes. Adhes.*, 2016, **64**, 65–71.
- 18 S. Sahoo, S. Mohanty and S. K. Nayak, *J. Macromol. Sci., Part A: Pure Appl. Chem.*, 2018, **55**, 36–48.
- 19 C. Zhang, T. F. Garrison, S. A. Madbouly and M. R. Kessler, *Prog. Polym. Sci.*, 2017, **71**, 91–143.
- 20 R. Vendamme and W. Eevers, *Macromolecules*, 2013, **46**, 3395–3405.
- 21 J. J. Gallagher, M. A. Hillmyer and T. M. Reineke, *ACS Sustainable Chem. Eng.*, 2016, **4**, 3379–3387.
- 22 S. Lee, K. Lee, Y.-W. Kim and J. Shin, *ACS Sustainable Chem. Eng.*, 2015, **3**, 2309–2320.
- 23 S. Panchireddy, B. Grignard, J.-M. Thomassin, C. Jerome and C. Detrembleur, *ACS Sustainable Chem. Eng.*, 2018, **6**, 14936–14944.
- 24 X. Zhang, M. C. D. Carter, M. E. Belowich, G. Wan, M. Crimmins, K. B. Laughlin, R. C. Even and T. H. Kalantar, *ACS Appl. Polym. Mater.*, 2019, **1**, 1317–1325.
- 25 E. Faure, C. Falentin-Daudré, C. Jérôme, J. Lyskawa, D. Fournier, P. Woisel and C. Detrembleur, *Prog. Polym. Sci.*, 2013, **38**, 236–270.
- 26 M. R. Thomsett, T. E. Storr, O. R. Monaghan, R. A. Stockman and S. M. Howdle, *Green Mater.*, 2016, **4**, 115–134.
- 27 P. A. Wilbon, F. Chu and C. Tang, *Macromol. Rapid Commun.*, 2013, **34**, 8–37.
- 28 M. Winnacker and B. Rieger, *ChemSusChem*, 2015, **8**, 2455–2471.
- 29 M. F. Sainz, J. A. Souto, D. Regentova, M. K. G. Johansson, S. T. Timhagen, D. J. Irvine, P. Buijsen, C. E. Koning, R. A. Stockman and S. M. Howdle, *Polym. Chem.*, 2016, **7**, 2882–2887.
- 30 S. Bloembergen, L. J. McLennan, S. E. Cassar and R. Narayan, *Adhes. Age*, 1998, **41**, 20.
- 31 J. Shin, Y. Lee, W. B. Tolman and M. A. Hillmyer, *Biomacromolecules*, 2012, **13**, 3833–3840.
- 32 J. Shin, M. T. Martello, M. Shrestha, J. E. Wissinger, W. B. Tolman and M. A. Hillmyer, *Macromolecules*, 2011, **44**, 87–94.
- 33 M. A. Driesbeke and F. E. Du Prez, *ACS Sustainable Chem. Eng.*, 2019, **7**, 11633–11639.
- 34 S. S. Baek, S. H. Jang and S. H. Hwang, *J. Ind. Eng. Chem.*, 2017, **53**, 429–434.
- 35 S.-S. Baek and S.-H. Hwang, *Eur. Polym. J.*, 2017, **92**, 97–104.
- 36 S. Noppalit, A. Simula, N. Ballard, X. Callies, J. M. Asua and L. Billon, *Biomacromolecules*, 2019, **20**, 2241–2251.
- 37 S. Noppalit, A. Simula, L. Billon and J. M. Asua, *Polym. Chem.*, 2020, **11**, 1151–1160.
- 38 Nitto Europe NV, Nitto Europe N.V. Sustainability Page, [https://www.nitto.com/eu/en/about\\_us/sustainability/](https://www.nitto.com/eu/en/about_us/sustainability/). (Accessed February 10<sup>th</sup>, 2020).
- 39 S. Molina-Gutiérrez, V. Ladmiral, R. Bongiovanni, S. Caillol and P. Lacroix-Desmazes, *Green Chem.*, 2019, **21**, 36–53.
- 40 R. Jovanović and M. A. Dubé, *J. Macromol. Sci., Part C: Polym. Rev.*, 2004, **44**, 1–51.
- 41 A. Matsumoto, N. Murakami, H. Aota, J. Ikeda and I. Capek, *Polymer*, 1999, **40**, 5687–5690.
- 42 F. Boscán, M. Paulis and M. J. Barandiaran, *Eur. Polym. J.*, 2017, **93**, 44–52.
- 43 S. Bunker, C. Staller, N. Willenbacher and R. Wool, *Int. J. Adhes. Adhes.*, 2003, **23**, 29.
- 44 R. P. Wool and S. P. Bunker, *J. Adhes.*, 2007, **83**, 907–926.
- 45 G. Palmese, J. La Scala and J. Sands, *US Pat*, 2005250923A1, 2005.
- 46 P. Hyde, *US Pat*, 2007276108A1, 2007.
- 47 R. P. Wool and S. P. Bunker, *US Pat*, 2002188056A1, 2002.
- 48 Y.-Y. Lu and K. S. Anderson, *W.O. Pat*, 2010075387A2, 2010.
- 49 C. Koch and S. Pathak, *W.O. Pat*, 2013154610A1, 2013.
- 50 J. Zhang, S. Severtson and L. Roerdink, *US Pat*, 2015210907A1, 2015.
- 51 S. Molina-Gutiérrez, V. Ladmiral, R. Bongiovanni, S. Caillol and P. Lacroix-Desmazes, *Ind. Eng. Chem. Res.*, 2019, **58**, 21155–21164.
- 52 S. Noppalit, A. Simula, L. Billon and J. M. Asua, *ACS Sustainable Chem. Eng.*, 2019, **7**, 17990–17998.
- 53 J. M. Asua, *Prog. Polym. Sci.*, 2014, **39**, 1797–1826.
- 54 G. E. Fonseca, T. F. McKenna and M. A. Dubé, *Chem. Eng. Sci.*, 2010, **65**, 2797–2810.
- 55 M. M. Rahaman Mollick, B. Bhowmick, D. Mondal, D. Maity, D. Rana, S. K. Dash, S. Chattopadhyay, S. Roy, J. Sarkar, K. Acharya, M. Chakraborty and D. Chattopadhyay, *RSC Adv.*, 2014, **4**, 37838–37848.
- 56 P. Sarkar and A. K. Bhowmick, *J. Polym. Sci., Part A: Polym. Chem.*, 2017, **55**, 2639–2649.
- 57 P. Sarkar and A. K. Bhowmick, *ACS Sustainable Chem. Eng.*, 2016, **4**, 2129–2141.
- 58 W. Lei, X. Yang, H. Qiao, D. Shi, R. Wang and L. Zhang, *Eur. Polym. J.*, 2018, **106**, 1–8.
- 59 P. Sahu and A. K. Bhowmick, *Ind. Eng. Chem. Res.*, 2019, **58**, 20946–20960.
- 60 P. Sahu, P. Sarkar and A. K. Bhowmick, *ACS Sustainable Chem. Eng.*, 2017, **5**, 7659–7669.
- 61 A. J. Back and F. J. Schork, *J. Appl. Polym. Sci.*, 2007, **103**, 819–833.
- 62 A. Badía, J. Movellan, M. J. Barandiaran and J. R. Leiza, *Ind. Eng. Chem. Res.*, 2018, **57**, 14509–14516.
- 63 A. Badía, J. I. Santos, A. Agirre, M. J. Barandiaran and J. R. Leiza, *ACS Sustainable Chem. Eng.*, 2019, **7**, 19122–19130.
- 64 L. Zhang, Y. Cao, L. Wang, L. Shao and Y. Bai, *J. Appl. Polym. Sci.*, 2016, **133**, 1.
- 65 A. J. J. Straathof, S. Sie, T. T. Franco and L. A. M. van der Wielen, *Appl. Microbiol. Biotechnol.*, 2005, **67**, 727–734.
- 66 A. J. J. Straathof, *Chem. Rev.*, 2014, **114**, 1871–1908.
- 67 C. V. Pramod, R. Fauziah, K. Seshan and J.-P. Lange, *Catal. Sci. Technol.*, 2018, **8**, 289–296.
- 68 E. Mehravar, M. A. Gross, A. Agirre, B. Reck, J. R. Leiza and J. M. Asua, *Eur. Polym. J.*, 2018, **98**, 63–71.



- 69 N. Ballard, J. C. de la Cal and J. M. Asua, *Macromolecules*, 2015, **48**, 987–993.
- 70 J. Chauvet, J. M. Asua and J. R. Leiza, *Polymer*, 2005, **46**, 9555–9561.
- 71 C. Plessis, G. Arzamendi, J. M. Alberdi, M. Agnely, J. R. Leiza and J. M. Asua, *Macromolecules*, 2001, **34**, 6138–6143.
- 72 C. Plessis, G. Arzamendi, J. R. Leiza, J. M. Alberdi, H. A. S. Schoonbrood, D. Charmot and J. M. Asua, *J. Polym. Sci., Part A: Polym. Chem.*, 2001, **39**, 1106.
- 73 N. Ballard and J. M. Asua, *Prog. Polym. Sci.*, 2018, **79**, 40–60.
- 74 J. H. Lee, T. H. Lee, K. S. Shim, J. W. Park, H. J. Kim, Y. Kim and S. Jung, *Int. J. Adhes. Adhes.*, 2017, **74**, 137.
- 75 C. M. Alder, J. D. Hayler, R. K. Henderson, A. M. Redman, L. Shukla, L. E. Shuster and H. F. Sneddon, *Green Chem.*, 2016, **18**, 3879–3890.
- 76 H. Sardon, L. Irusta, M. J. Fernández-Berridi, J. Luna, M. Lansalot and E. Bourgeat-Lami, *J. Appl. Polym. Sci.*, 2011, **120**, 2054–2062.
- 77 C.-H. Yang, S.-M. Lin and T.-C. Wen, *Polym. Eng. Sci.*, 1995, **35**, 722–730.
- 78 C. Chinwanitcharoen, S. Kanoh, T. Yamada, S. Hayashi and S. Sugano, *J. Appl. Polym. Sci.*, 2004, **91**, 3455–3461.
- 79 R. Salazar, P. Ilundain, D. Alvarez, L. Da Cunha, M. J. Barandiaran and J. M. Asua, *Ind. Eng. Chem. Res.*, 2005, **44**, 4042–4050.
- 80 E. P. Chang, *J. Adhes.*, 1997, **60**, 233–248.
- 81 E. P. Chang, in *Fundamentals of Pressure Sensitivity*, 5th edn, 2009, ch. 5, pp. 5-1–5-18.
- 82 Y. Peykova, O. V. Lebedeva, A. Diethert, P. Müller-Buschbaum and N. Willenbacher, *Int. J. Adhes. Adhes.*, 2012, **34**, 107–116.
- 83 A. Kowalski, Z. Czech and Ł. Byczyński, *J. Coat. Technol. Res.*, 2013, **10**, 879–885.
- 84 A. Agirre, J. Nase, E. Degrandi, C. Creton and J. M. Asua, *J. Polym. Sci., Part A: Polym. Chem.*, 2010, **48**, 5030.